HHS Public Access

Author manuscript

Nat Struct Mol Biol. Author manuscript; available in PMC 2012 December 01.

Published in final edited form as:

Nat Struct Mol Biol. ; 19(6): 628–632. doi:10.1038/nsmb.2295.

Structural basis for cisplatin DNA damage tolerance by human polymerase η during cancer chemotherapy

Ajay Ummat[1], **Olga Rechkoblit**[1], **Rinku Jain**[1], **Jayati R. Choudhary**[2], **Robert E. Johnson**[2], **Timothy D. Silverstein**[1], **Angeliki Buku**[1], **Samer Lone**[1], **Louise Prakash**[2], **Satya Prakash**[2], and **Aneel K. Aggarwal**[1]

[1]Department of Structural & Chemical Biology, Mount Sinai School of Medicine, Box 1677, 1425 Madison Avenue, New York, NY 10029.

[2]Department of Biochemistry and Molecular Biology, 301 University Blvd., University of Texas Medical Branch, Galveston, TX 77755-1061.

Abstract

A major clinical problem in the use of cisplatin to treat cancers is tumor resistance. DNA polymerase η (Polη) is a key polymerase that allows cancer cells to cope with cisplatin–DNA adducts formed during chemotherapy. We present here a structure of human Polη inserting dCTP opposite a cisplatin intrastrand cross-link (PtGpG). We show that specificity of human Polη for PtGpG derives from an active site that is open to permit Watson-Crick geometry of the nascent PtGpG•dCTP base pair and to accommodate the lesion without steric hindrance. The specificity is augmented by residues Gln38 and Ser62 that interact with PtGpG, and Arg61 that interacts with incoming dCTP. Collectively, the structure provides a basis for understanding how Polη in human cells can tolerate DNA damage caused by cisplatin chemotherapy and offers a framework for the design of inhibitors in cancer therapy.

Introduction

Cisplatin and related analogues are the mainstay of modern cancer chemotherapy. Approved by the FDA in 1978, cisplatin has been used to treat a variety of cancers, from ovarian and cervical to non-small cell lung, among others[1,2]. The cytotoxicity of cispaltin towards cancer cells derives from its impediment to processes such as DNA replication and transcription, leading to cellular apoptosis. In particular, the platinum atom binds covalently to the N7 position of adjacent guanines to form 1, 2 intrastrand crosslinks (PtGpG) (Fig. 1a), which cannot be bypassed by the classic replicative DNA polymerases (Polα, Polδ and Polε) and

Correspondence should be addressed to A.K.A (aneel.aggarwal@mssm.edu).

Accession codes. Coordinates and structure factors have been deposited into the Protein Data Bank under the accession code 4EEY.

AUTHOR CONTRIBUTIONS A.K.A and A.U designed the experiments; A.U determined the crystal structure; O.R and A.U prepared the cisplatin adduct; R.J assisted in the crystallographic analysis; T.D.S and S.L assisted in DNA preparation; A.B assisted in protein purification; J.R.C. and R.E.J performed the biochemical experiments; L.P and S.P guided the biochemical studies; A.K.A wrote the manuscript with contributions from all of the authors.

Competing Financial Interests The authors declare no competing financial interests

DNA synthesis comes to a halt. A major drawback in the use of cisplatin, however, is acquired or intrinsic tumor resistance during the courses of therapy[3]. This resistance can be mediated by a number of cellular processes, including translesion DNA synthesis (TLS)[1,4].

Humans possess four TLS polymerases - Polη, Polκ, Polι and Rev1 – each with a unique DNA damage bypass and fidelity profile [5]. Polη is unique amongst these in its ability to replicate through ultraviolet (UV)-induced intrastrand crosslinked *cis-syn* thymine– thymine (T–T) dimers[6]. Inactivation of Polη in humans causes the variant form of xeroderma pigmentosum (XP-V)[6,7], a genetic disorder characterized by a greatly enhanced predisposition to sun induced skin cancers. Crystal structures of yeast *Saccharomyces cerevisiae* and human Polη with undamaged and UV-damaged DNAs show that the Polη active site cleft is more open or spacious than in other DNA polymerases[8,9], allowing a *cis-syn* T-T dimer to be accommodated within it.

In addition to its role in suppressing skin cancers, Polη has also emerged as the main TLS polymerase that allows cancer cells to cope with cisplatin-DNA adducts formed during cancer chemotherapy. Polη bypasses Pt-GpG crosslinks more efficiently than other polymerases[10-12], and the absence of functional Polη in XP-V cells correlates with the sensitivity of these cells to cisplatin [10,11,13]. In addition, endogenous Polη level has been found to be reliable marker of cisplatin efficacy in non-small cell lung cancer cell lines[14]. As such, Polη is a novel target for cancer therapy, whereby inhibiting it may increase the efficacy of traditional cisplatin chemotherapy.

How human Polη bypasses cisplatin-DNA adducts during TLS remains unclear. A medium resolution crystal structure of yeast Polη bound to a cisplatin-DNA adduct has been reported but a number of structural features remain unclear[9,15]. We report here a high-resolution crystal structure of the catalytic domain of human Polη inserting dCTP opposite the 3′G of a PtGpG crosslink. The structure provides a molecular basis for understanding how Polη in human cells can tolerate DNA damage caused by cisplatin chemotherapy and offers a framework for the design of inhibitors in future cancer therapy.

RESULTS

Structure determination

The catalytic core of human Polη (residues 1 to 432) was cocrystallized with a 9-nt/13-nt primer/template presenting the 3′G of a PtGpG adduct as templating base and with dCTP as the incoming nucleotide. The cisplatin modification was introduced between two adjacent guanines in the template strand (5′ – CTT**GG**TCTCCTCC – 3′) by the method described by Gelasco and Lippard[16]. Several rounds of micro-seeding were required to produce good quality cocrystals, which diffracted to 2.32Å resolution with synchrotron radiation at the L_{III} absorption edge of platinum (λ =1.0722 Å). The structure was solved by the molecular replacement (MR) method, using the human Polη ternary structure with undamaged DNA as the search model (PDB 3MR2)[8]. The refined model includes residues 2 to 432 of the protein (residues 156 and 157 and 410-412 could not be modeled due to lack of electron density), nucleotides 2 to 9 of the primer strand, nucleotides 4 to 13 of the template strand, one dCTP molecule, one magnesium ion, and 116 water molecules (Table 1). The structure has good

stereochemistry (Fig. 1), with 97.9% of the residues in the most favored regions of the Ramachandran plot, based on MolProbity Ramachandran analysis[17].

As with undamaged DNA[8], human Polη embraces the PtGpG template-primer with its palm, fingers, and thumb domains, as well as the polymerase associated domain (PAD; also known as the little finger domain) unique to Y-family polymerases (Fig. 1b–c). The palm carries the active site residues, Asp13, Asp115 and Glu116, which catalyze the nucleotidyl transfer reaction upon dNTP binding. The fingers domain lies above the templating PtGpG•dCTP base pair, while the thumb and the PAD straddle the duplex portion of the template-primer (Fig. 1b–c). The thumb skims the minor groove surface of the DNA, making contacts with the sugar-phosphate backbone of the primer strand. The PAD docks in the major groove and interacts extensively with the template and primer strands (Supplementary Fig. 1). In particular, the main chain amides on the "outer" β-strands of the PAD β-sheet make a series of hydrogen bonds with the sugar-phosphate backbones of the template and primer strands. The DNA remains essentially B-form except at the site of the PtGpG adduct (Fig. 1). The average DNA helical twist and rise values are 32.7° and 3.3Å, respectively.

Cisplatin resides in an open active cleft

Even though PtGpG is a larger and a more distorted DNA crosslink than a UV-induced *cis-syn* T-T dimer (Fig. 1), human Polη accommodates this bulky lesion remarkably well with only a small (~1Å) outward movement of the fingers domain, when compared to human Polη structures with undamaged and UV damaged DNAs[8] (Fig. 2a–b). Thus, as in the case of UV-damaged DNA, the key feature of human Polη that allows it to accommodate a cisplatin intrastrand cross-link is an active site cleft that is more open than in other DNA polymerases, including other TLS polymerases. Figure 2c–e shows the structure of human Polκ superimposed onto that of human Polη (via their palm domains; residues 90-238 in human Polη and 171-338 in human Polκ). In contrast to human Polη, human Polκ's fingers domain and the N-terminal segment (N-clasp) sterically overlap with the 5′G of PtGpG (Fig. 2c–e). Human Polκ would thus require a larger conformational rearrangement than human Polη to accommodate a PtGpG adduct. The steric clashes are even more severe if the two polymerases are superimposed based on their respective template DNA strands (Supplementary Fig. 3). In addition, the human Polη active site cleft contains residues that make specific interactions with the PtGpG adduct (Fig. 3a). The 3′G of PtGpG is stabilized by a hydrogen bond between its N3 atom and the Nε2 amino group of Gln38; analogous to the hydrogen bond between the O2 carbonyl of the 3′T of the T-T dimer and Nε2 of Gln38 in the structure of human Polη with UV-damaged DNA[8] (Fig. 3). Accordingly, a Q38A mutation confers an ~2-3 fold reduction in the catalytic efficiency of human Polη for the incorporation of dCTP opposite the 3′G of PtGpG (Supplementary Fig. 3 and Supplementary Table 1), analogous to the ~2-fold reduction in catalytic efficiency of the polymerase observed opposite the 3′T of a T-T dimer[8]. The 5′G of PtGpG is almost perpendicular to the 3′G and lies towards the outside edge of hPolη active site cleft - in intimate contact with Ser62 (Fig. 3a). As such, the position and orientation of the 5′G is different from the 5′T of a T-T dimer (Fig. 2b), which is less angularly inclined and fits directly within active site cleft - further away from Ser62. Since the 5′G of PtGpG resides towards the periphery of the active site cleft there are no direct interactions with Arg61,

analogous to those with the 5′T of a T-T dimer. That is, whereas Arg61 assumes three rotamers in the structure with a T-T dimer[8], one of which interacts with the 5′T and others with incoming dATP (Fig. 3b), Arg61 assumes a single conformation with PtGpG and interacts exclusively with incoming dCTP (Fig. 3a). This difference may underlie the milder effect of the R61A mutation for the incorporation of dCTP opposite the 3′G of PtGpG (Supplementary Fig. 3 and Supplementary Table 1), compared to the ~2.5 fold reduction in catalytic efficiency observed opposite the 3′T of a T-T dimer[8]. The most striking effect is observed for the Q38A R61A double mutant, where dCTP incorporation is reduced by ~10-fold opposite the 3′G on both undamaged and PtGpG DNA (Supplementary Fig. 3 and Supplementary Table 1). Collectively, based on our structural and biochemical observations, we infer an important role for Gln38 and Arg61 in the bypass of PtGpG adduct by human Polη.

Error-free bypass

The 3′G of PtGpG makes an almost perfect Watson-Crick base pair with incoming dCTP (Fig. 3a), with relatively low propeller twist (~0.4°) between the bases and classical hydrogen bonds between O6, N1, and N2 of G and N4, N3, and O2 of C, respectively. At the same time, the triphosphate moiety of dCTP is interlaced between the fingers and palm domains and makes hydrogen bonds with Tyr52 and Arg55 from the fingers domain and Lys231 from the palm domain (Fig. 3a). The catalytic residues Asp13, Asp115 and Glu116 are arrayed between the dCTP triphosphate and the primer terminus. Curiously, there is one Mg^{2+} ion at a position analogous to “metal B” in DNA polymerases, as compared to two Mg^{2+} ions in previous human Polη structures[8] (Fig. 3). This is probably because the primer in our structure contains a dideoxy terminus, as compared to a deoxy terminus in previous human Polη structures. Nonetheless, the putative 3′OH (at the primer terminus) in our structure is located ~ 3.1Å from the dCTP α-phosphate and aligned with respect to the Pα-O3′ bond (angle of ~160°) for an in-line nucleophilic attack – leading to the incorporation of C opposite the 3′G of the PtGpG adduct.

DISCUSSION

A major clinical problem in the use of cisplatin to treat cancers is tumor resistance[1,3]. The ability of human Polη to bypass cisplatin-DNA adducts formed during cancer chemotherapy is one important mechanism by which tumors appear to gain such resistance[4]. We show here that human Polη can accommodate a bulky PtGpG DNA crosslink within its active site cleft without any major rearrangement of the enzyme. The specificity of human Polη for PtGpG, as compared to other DNA polymerases, derives from an active site cleft that is sufficiently open to permit not only near perfect Watson-Crick geometry of the nascent PtGpG•dCTP base pair but also to accommodate the steeply inclined 5′G of PtGpG without any steric hindrance. The specificity for PtGpG is further augmented by residues Gln38 and Ser62 that interact with the 3′G and 5′G of the PtGpG adduct, respectively, and Arg61 that interacts with incoming dCTP. Amongst human TLS polymerases[5], Arg61 and Ser62 are unique to Polη, while Gln38 occurs only in Polη and Pol⌊. In the structure of yeast Polη in complex with a cisplatin-DNA adduct, Gln55 and Arg73 make similar local interactions with DNA as Gln38 and Arg61 in human Polη. By contrast, in the structure of prokaryotic Dpo4–PtGpG

complex that lacks these amino acids, the 3′G is tilted and shifted towards the major groove and unable to make a WC base pair with incoming dCTP[18]. Thus, interactions with Gln38 and Ser62 appear to be necessary to keep the PtGpG optimally oriented for proper WC base pairing between 3′G and incoming dCTP.

The human Polη active site cleft is well-poised for catalysis and for incorporation of C opposite the 3′G of PtGpG. Thus, even though PtGpG is a larger and more distorted intrastrand cross-link than a *cis-syn* T-T dimer, it does not lead to any significant perturbation of the human Polη active site or impact the ability of the polymerase to carry out catalysis. The primer terminus is well-aligned for incorporation of C opposite the 3′G of PtGpG adduct. By contrast, based on our biochemical studies, human Polη is markedly inhibited in extending from the 3′G, 5′G, or the next templating residue of the PtGpG adduct (Supplementary Fig. 3). This may be one reason why we were unsuccessful in obtaining suitable crystals of a ternary complex of human Polη inserting a nucleotide opposite the 5′G of the PtGpG adduct. A recurring theme in TLS is that lesion bypass often requires the sequential action of two polymerases, an “inserter” and an “extender”[5].

The inserter is efficient at insertion of an incoming nucleotide across from the lesion and the extender is recruited to add bases downstream of the lesion. In eukaryotes, Polζ, a B-family polymerase, is specialized for the extension step of lesion bypass[19], and it is conceivable that Polζ (or another polymerase) is recruited in human cells to complete PtGpG bypass.

The ability of human Polη to replicate across from a cisplatin adduct makes it an attractive target for cancer therapy. A pressing question is whether one can design or identify inhibitors that are specific for human Polη ? The fact that the shape of the human Polη active site cleft is different from that of other DNA polymerases suggest that it would be possible to derive small molecules that can specifically inhibit human Polη. The human Polη active site cleft, for example, is more open than in other DNA polymerases and it lacks elements such as the N-clasp in human Polκ and the N-digit in human Rev1[20,21]. At the same time, the presence of unique (Arg61 and Ser62) and nearly unique (Gln38) residues within the active site cleft offer the possibility of specific hydrogen bonds with unique small molecules.

ONLINE METHODS

Preparation of protein and DNA for crystallization—The catalytic core of human Polη (residues 1–432) harboring an N-terminal hexa-histadine (6XHis) tag and a C406M mutation was overexpressed in *Escherichia coli* and purified as previously described by Biertumpfel et al[8]. Briefly, the 6XHis tag was removed via overnight incubation with PreScission protease and the protein subsequently purified via ion-exchange (MonoS) and size-exclusion (Superdex75) chromatography, prior to concentration of the protein for crystallization experiments. A HPLC purified 13–nt template strand (5′ – CTT**GG**TCTCCTCC – 3′) was prepared (Integrated DNA Technologies Inc.) and a *cis*-Diamminedichloroplatinum(II) (cisplatin; GFS Chemicals Inc.) intrastrand d(GpG) cross-link introduced between the two adjacent guanines based on the method described by Gelasco and Lippard[16]. The cisplatin modified template strand was further purified by HPLC on a reversed-phase C18 column (Waters Inc.) A 9–nt primer strand harboring a

dideoxyadenosine at its 3′ end (5′ –TGGAGGAGA^{dd} - 3′) was annealed in the molar ratio of 1:1 to the 13–nt cisplatin-modified template strand to yield the 9–nt/13–nt primer/template.

Preparation of proteins for biochemical analysis—The full length wild-type and the various mutant versions of human Polη were expressed in yeast *Saccharomyces cerevisiae* and purified by glutathione-Sepharose affinity chromatography as described previously[22], except that proteins contained tandem N-terminal GST and Flag tags. The GST tags were removed by treatment with PreScission protease, leaving an N-terminal Flag tag attached to each protein. Proteins were quantified by Coomassie stained SDS-PAGE analysis. Mutations were introduced into the wild type open reading frame by PCR using oligonucleotides containing site specific mutations and were confirmed by sequencing prior to expression.

DNA polymerase assays—DNA substrates consisted of a radiolabeled oligonucleotide primer annealed to a 78-nt oligonucleotide DNA template by heating a mixture of primer/template at a 1:1.5 molar ratio to 95°C and allowing it to cool to room temperature for several hours. The template 78-mer oligonucleotide contained the sequence 5′AGCAAGTCAC CAATGTCTAA GAGTTTCTTGGTCTCCTCCT ACACTGGAGT ACCGGAGCAT CGTCGTGACT GGGAAAAC-3′ and was either undamaged or harbored a G-Pt-G intrastrand cross-link at the underlined position. The sequence of the running start primer is 5′CGACGATGCTCCGGTACTCCAGTGTAG 3′. For steady-state kinetic analyses of nucleotide insertion opposite the 3′G of either the undamaged GG or GG cisplatin template, the primer 5′GATGCTCCGG TACTCCAGTG TAGGAGGAGA 3′ was used. The standard DNA polymerase reaction (5 μl) contained 25 mM Tris·HCl (pH 7.5), 5 mM $MgCl_2$, 1 mM dithiolthreitol, 100 μg ml^{-1} BSA, 10% glycerol, and 10 nM DNA substrate. For running start assays, 25 μM each of dATP, dTTP, dCTP, and dGTP (Roche Biochemicals) was included. For steady state kinetic experiments, only dCTP was included at concentrations ranging from 0.05 to 50 μM. Reactions containing wild type and mutant Polη (0.05 nM to 0.5 nM) were carried out at 37 °C for 5-10 min. Reactions were terminated by the addition of 6 volumes of loading buffer (95% formamide, 0.05% cyanol blue, and 0.05% bromophenol blue) before resolving on 12% polyacrylamide gels containing 8M urea. Gels were dried before autoradiography.

Steady-state kinetic analysis—Steady-state kinetic analyses for deoxynucleotide incorporation were performed as described[22]. Gel band intensities of the substrate and products of the deoxynucleotide incorporation reactions were quantified by using a PhosphorImager and the IMAGEQUANT software (Molecular Dynamics). The observed rate of deoxynucleotide incorporation, v_{obs} was determined by dividing the amount of product formed by the reaction time and protein concentration. The v_{obs} was graphed as a function of the deoxynucleotide concentration, and the data were fit to the Michaelis-Menten equation describing a hyperbola: $v_{obs} = (k_{cat}[E] \times [dNTP])/(K_m + [dNTP])$. From the best fit curve, the apparent K_m and k_{cat} steady-state kinetics parameter were obtained for the incorporation of dCTP by the wild type and mutant Polη and the efficiencies of nucleotide incorporation (k_{cat}/K_m) determined.

Cocrystallization—The cisplatin (PtGpG) ternary complex was prepared by mixing human Polη with the cisplatin modified primer/template in a 1:1.1 molar ratio in the presence of 2mM dCTP and 5mM $MgCl_2$. This mix was incubated for at least an hour before crystallization. Thin needle-like crystals were obtained in 0.1M Bis-Tris (pH 5.5) and 30%-35% (w/v) of PEG 1500 by the vapor diffusion method at 20°C. Several rounds of microseeding (15-30% PEG 1500) were required to produce good quality crystals. For data collection, the crystals were cryoprotected by step-wise soaks for 5 min in mother liquor solutions containing 5-30% (v/v) of glycerol, and then flash frozen in liquid nitrogen. X-ray diffraction data were collected on beamline X25 at Brookhaven National Laboratory (BNL). The crystals diffract to 2.32 Å resolution with synchrotron radiation at the platinum L_{III} absorption edge (λ = 1.0722 Å). Crystals belong to space group P6(1) with unit cell dimensions a = 98.5 Å, b = 98.5 Å and c = 82.6 Å. Matthew's coefficient calculation indicates one protein-DNA complex in the asymmetric unit.

Structure determination and refinement—The structure was solved by molecular replacement (MR), using the human Polη ternary structure (PDB 3MR2), with the DNA, incoming nucleotide, metals, and water molecules omitted, as the starting model[8]. The program PHASER gave a unique MR solution[23]. The first round of refinement and map calculation was carried out with just the enzyme using REFMAC[24]. The electron density maps (2Fo-Fc and Fo-Fc) showed unambiguous densities for the cisplatin 1, 2 intrastrand crosslink between the adjacent guanines in the template strand (Fig. 1d–e), primer strand, incoming nucleotide and metal, which were then iteratively built into the map using COOT[25]. Iterative rounds of refinement and water picking were performed with REFMAC, and model building with COOT. The final model has excellent stereochemistry (Fig. 1), as shown by Molprobity with 97.9% of the residues in the most favored regions of the Ramachandran plot[17]. Figures were prepared using PyMol (http://www.pymol.org)

Supplementary Material

Refer to Web version on PubMed Central for supplementary material.

ACKNOWLEDGMENTS

We thank the staff at BNL (beamline X25) for facilitating X-ray data collection. We also thank G. Gerona-Navarro for assistance with HPLC. This work was supported by grants ES017767 and ES012411 from the National Institutes of Health (NIH). A. Ummat was supported in part by NIH training grant T32 GM62754

References

1. Kelland L. The resurgence of platinum-based cancer chemotherapy. Nat Rev Cancer. 2007; 7:573–84. [PubMed: 17625587]
2. Wang D, Lippard SJ. Cellular processing of platinum anticancer drugs. Nat Rev Drug Discov. 2005; 4:307–20. [PubMed: 15789122]
3. Kartalou M, Essigmann JM. Mechanisms of resistance to cisplatin. Mutat Res. 2001; 478:23–43. [PubMed: 11406167]
4. Lord CJ, Ashworth A. The DNA damage response and cancer therapy. Nature. 2012; 481:287–94. [PubMed: 22258607]
5. Prakash S, Johnson RE, Prakash L. Eukaryotic Translesion Synthesis DNA Polymerases: Specificity of Structure and Function. Annu Rev Biochem. 2005; 74:317–353. [PubMed: 15952890]

6. Johnson RE, Prakash S, Prakash L. Efficient bypass of a thymine-thymine dimer by yeast DNA polymerase, Poleta. Science. 1999; 283:1001–4. [PubMed: 9974380]
7. Masutani C, et al. The XPV (xeroderma pigmentosum variant) gene encodes human DNA polymerase eta [see comments]. Nature. 1999; 399:700–4. [PubMed: 10385124]
8. Biertumpfel C, et al. Structure and mechanism of human DNA polymerase eta. Nature. 2010; 465:1044–8. [PubMed: 20577208]
9. Silverstein TD, et al. Structural basis for the suppression of skin cancers by DNA polymerase eta. Nature. 2010; 465:1039–43. [PubMed: 20577207]
10. Vaisman A, Masutani C, Hanaoka F, Chaney SG. Efficient translesion replication past oxaliplatin and cisplatin GpG adducts by human DNA polymerase eta. Biochemistry. 2000; 39:4575–80. [PubMed: 10769112]
11. Chen YW, Cleaver JE, Hanaoka F, Chang CF, Chou KM. A novel role of DNA polymerase eta in modulating cellular sensitivity to chemotherapeutic agents. Mol Cancer Res. 2006; 4:257–65. [PubMed: 16603639]
12. Bassett E, et al. Efficiency of extension of mismatched primer termini across from cisplatin and oxaliplatin adducts by human DNA polymerases beta and eta in vitro. Biochemistry. 2003; 42:14197–206. [PubMed: 14640687]
13. Albertella MR, Green CM, Lehmann AR, O'Connor MJ. A role for polymerase eta in the cellular tolerance to cisplatin-induced damage. Cancer Res. 2005; 65:9799–806. [PubMed: 16267001]
14. Ceppi P, et al. Polymerase eta mRNA expression predicts survival of non-small cell lung cancer patients treated with platinum-based chemotherapy. Clin Cancer Res. 2009; 15:1039–45. [PubMed: 19188177]
15. Alt A, et al. Bypass of DNA lesions generated during anticancer treatment with cisplatin by DNA polymerase eta. Science. 2007; 318:967–70. [PubMed: 17991862]
16. Gelasco A, Lippard SJ. NMR solution structure of a DNA dodecamer duplex containing a cis-diammineplatinum(II) d(GpG) intrastrand cross-link, the major adduct of the anticancer drug cisplatin. Biochemistry. 1998; 37:9230–9. [PubMed: 9649303]
17. Davis IW, et al. MolProbity: all-atom contacts and structure validation for proteins and nucleic acids. Nucleic Acids Res. 2007; 35:W375–83. [PubMed: 17452350]
18. Wong JH, et al. Structural insight into dynamic bypass of the major cisplatin-DNA adduct by Y-family polymerase Dpo4. EMBO J. 2010; 29:2059–69. [PubMed: 20512114]
19. Johnson RE, Washington MT, Haracska L, Prakash S, Prakash L. Eukaryotic polymerases iota and zeta act sequentially to bypass DNA lesions. Nature. 2000; 406:1015–9. [PubMed: 10984059]
20. Nair DT, Johnson RE, Prakash L, Prakash S, Aggarwal AK. Rev1 employs a novel mechanism of DNA synthesis using a protein template. Science. 2005; 309:2219–22. [PubMed: 16195463]
21. Lone S, et al. Human DNA polymerase kappa encircles DNA: implications for mismatch extension and lesion bypass. Mol Cell. 2007; 25:601–14. [PubMed: 17317631]
22. Johnson RE, Prakash L, Prakash S. Yeast and human translesion DNA synthesis polymerases: expression, purification, and biochemical characterization. Methods Enzymol. 2006; 408:390–407. [PubMed: 16793382]
23. McCoy AJ, Grosse-Kunstleve RW, Storoni LC, Read RJ. Likelihood-enhanced fast translation functions. Acta Crystallogr D Biol Crystallogr. 2005; 61:458–64. [PubMed: 15805601]
24. Winn MD, Murshudov GN, Papiz MZ. Macromolecular TLS refinement in REFMAC at moderate resolutions. Methods Enzymol. 2003; 374:300–21. [PubMed: 14696379]
25. Emsley P, Cowtan K. Coot: model-building tools for molecular graphics. Acta Crystallogr D Biol Crystallogr. 2004; 60:2126–32. [PubMed: 15572765]

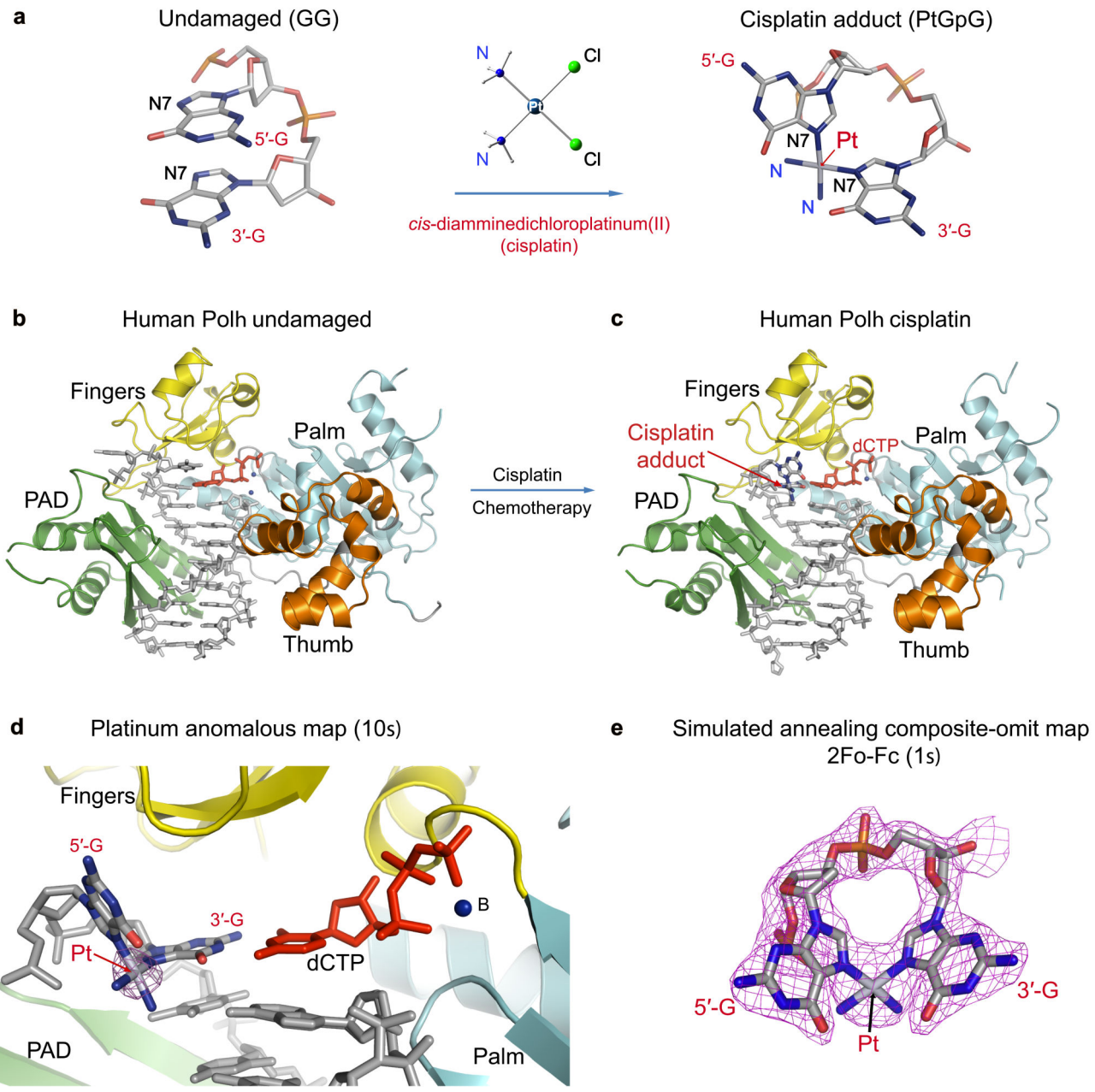

Figure 1.

Human Polη–DNA ternary complexes. **(a)** Schematic of cisplatin reaction with the N7 atoms of adjacent guanines to form a 1,2 intrastrand PtGpG cross-link. (**b**) Structure of human Polη in ternary complex with undamaged DNA and incoming dATP[8] (PDB 3MR2). The palm, fingers, thumb domains and the PAD are shown in cyan, yellow, orange and green, respectively. The DNA is in grey and the incoming dATP is in red. The putative Mg^{2+} ions are shown in dark blue. **(c)** Structure of human Polη in ternary complex with cisplatin intrastrand cross-link (PtGpG) DNA and incoming dCTP. The PtGpG is shown in grey and blue and incoming dCTP is shown in red. The putative Mg^{2+} ion is shown in dark blue. **(d)** Active site cleft of human Polη ternary complex bound to PtGpG crosslinked

DNA. The anomalous electron density for platinum is shown at the 10σ level. **(e)** Simulated annealed composite-omit 2Fo-Fc map (1.0σ) of PtGpG.

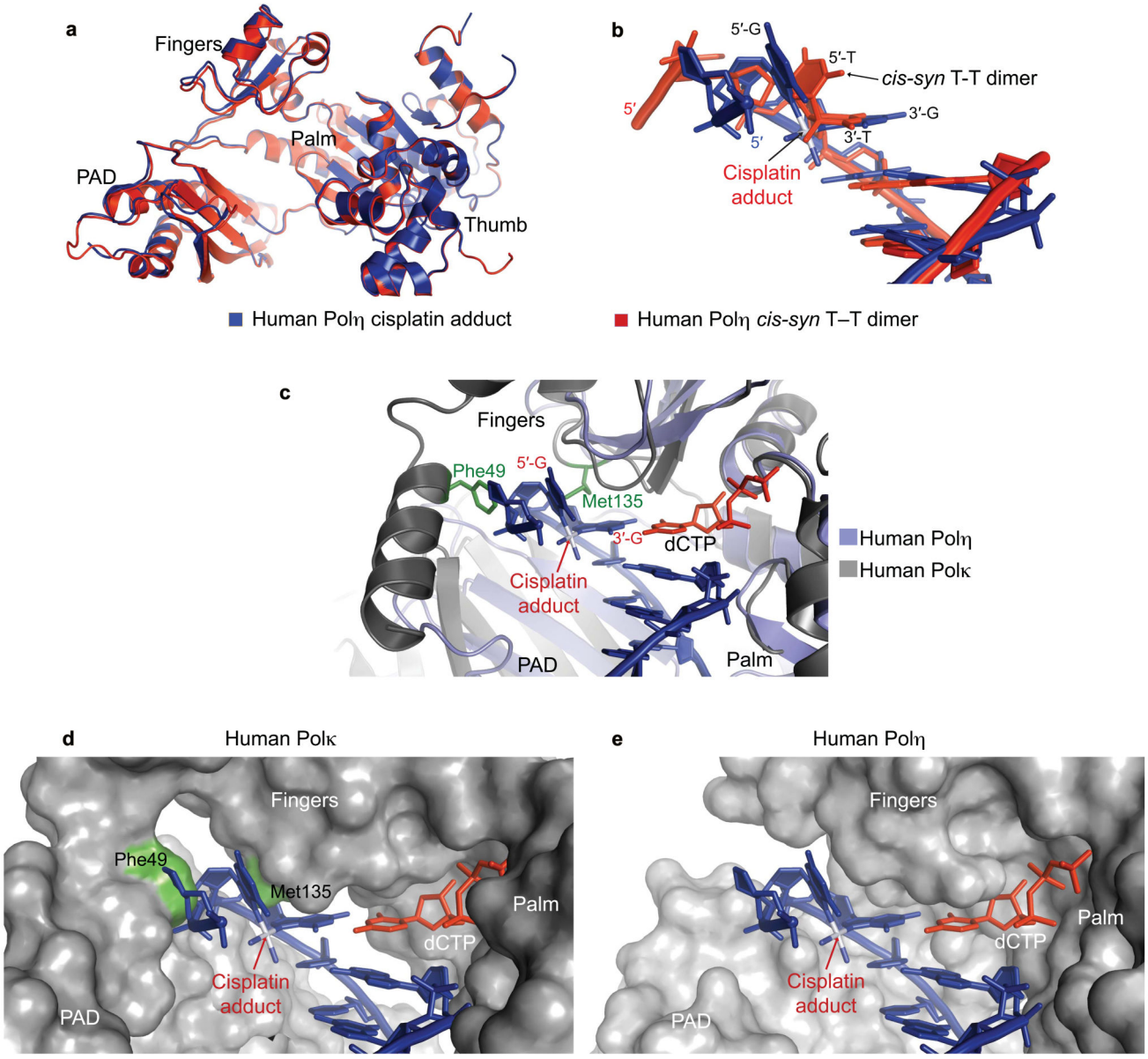

Figure 2.

Comparison of human Polη–PtGpG ternary complex with human Polη–T–T dimer and human Polκ–DNA complexes. **(a)** Human Polη in the *cis-syn* T-T dimer[8] (PDB 3MR3) and PtGpG complex is shown in red and blue, respectively. The two complexes are superimposed based on their palm domains. The superposition reveals subtle conformational changes in the fingers domain and the PAD. **(b)** Comparison of the DNA template and primer strands in the human Polη *cis-syn* T-T dimer (shown in red) and PtGpG ternary complexes (shown in blue). **(c)** Human Polη (blue) and human Polκ (grey) superimposed based on their palm domains. In human Polκ (PDB 2OH2)[21], the fingers domain is in close proximity to the PtGpG (dark blue) and it collides with the 5′G of the PtGpG. **(d)** Molecular surface of human Polκ when superimposed on the human Polη ternary complex via the palm

domains. The cisplatin intrastrand cross-link PtGpG sterically overlaps with Met135 of the fingers domain and other residues (Phe49) of N-clasp domain of Polκ. A change in Phe49 and Met135 rotamers would not relieve steric clashes with PtGpG (and leads to clashes with other human Polκ residues). **(e)** Molecular surface of human Polη in the PtGpG ternary complex. PtGpG fits unhindered within the active site cleft.

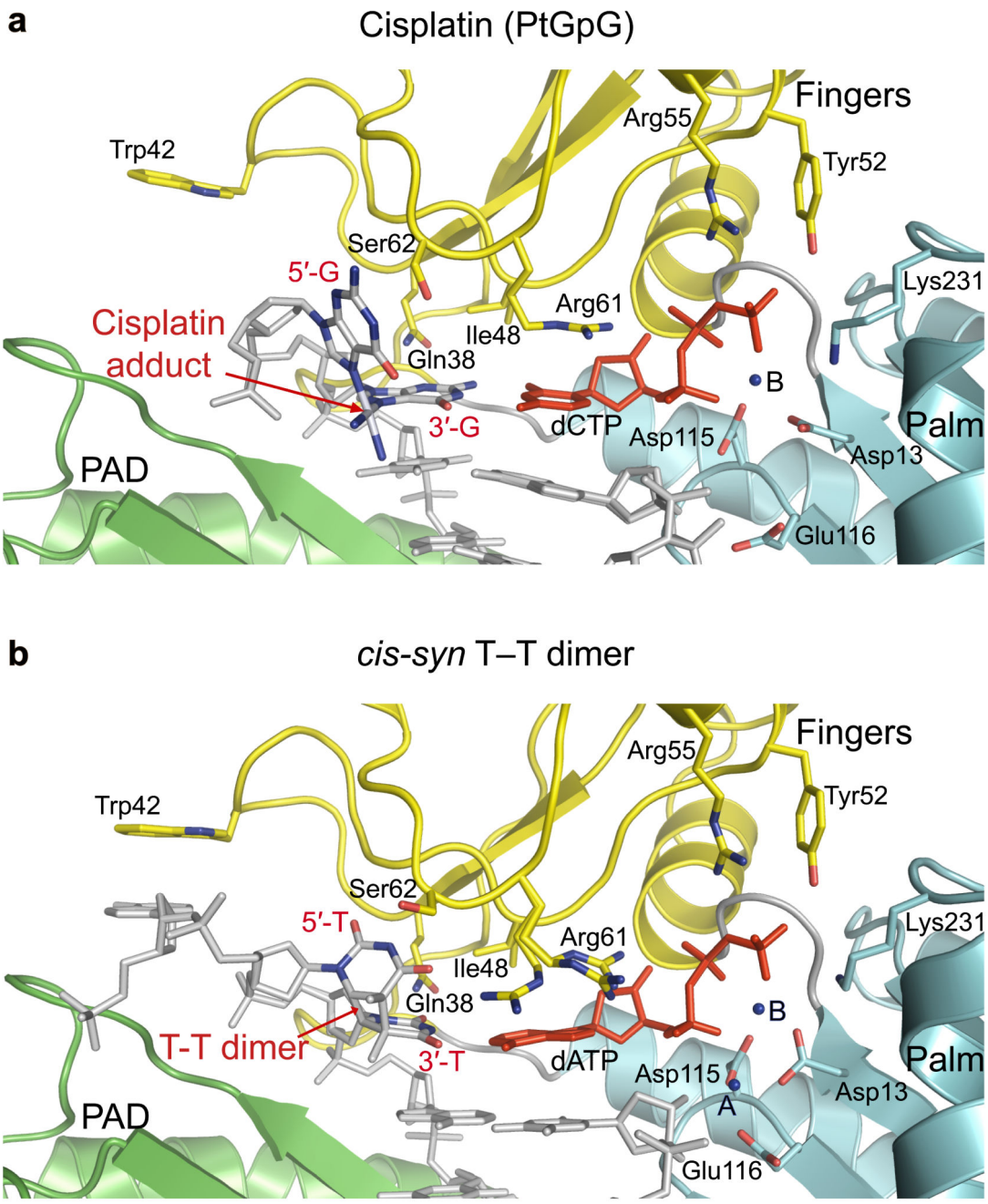

Figure 3.

Close-up views of the active site regions of human Polη ternary complexes bound to **(a)** PtGpG DNA, and **(b)** *cis-syn* T-T dimer DNA[8] (PDB 3MR3) The palm, fingers and PAD domains are shown in cyan, yellow and green, respectively. The DNA is colored grey, incoming nucleotide is in red and the putative Mg^{2+} ions are dark blue in both the structures. The residues are colored to match the color of their respective domains. Highlighted and labeled are the catalytic residues (Asp13, Asp115 and Glu116), and residues that interact with the triphosphate moiety of incoming nucleotide (Tyr52, Arg55). Arg61 has one

conformation in the PtGpG ternary complex where it interacts with the incoming dCTP, in contrast it adopts multiple conformations in the *cis-syn* T-T dimer ternary complex.

Table 1

Data collection and refinement statistics (molecular replacement)

	PtGpG human Polη
Data collection	
Space group	$P6_1$
Cell dimensions	
a, *b*, *c* (Å)	98.5, 98.5, 82.6
α, β, γ (°)	90.0, 90.0, 120.0
Resolution (Å)	50.0 - 2.3 (2.4 - 2.3)
R_{sym} or R_{merge}	10.8 (46.2)
I / σI	16.9 (3.8)
Completeness (%)	100 (99.9)
Redundancy	6.2 (5.2)
Refinement	
Resolution (Å)	49.2 - 2.3 (2.4 - 2.3)
No. reflections	18206 (1435)
R_{work} / R_{free} (%)	17.8 / 23.2
No. atoms	
Protein	3257
Ligand/ion	440
Water	116
B-factors (Å^2)	
Protein	49.0
Ligand/ion	54.9
Water	33.6
R.m.s. deviations	
Bond lengths (Å)	0.008
Bond angles (°)	1.134

Single crystal was used for solving the structure.

Values in parentheses are for highest-resolution shell.